NbN-Based Ferromagnetic 0 and π Josephson Junctions

Taro Yamashita, Akira Kawakami, and Hirotaka Terai

Phys. Rev. Applied **8**, 054028 — Published 14 November 2017

DOI: 10.1103/PhysRevApplied.8.054028

NbN-based 0 and π ferromagnetic Josephson junctions

Taro Yamashita,[1,2,*] Akira Kawakami,[1] and Hirotaka Terai[1]

1. *Advanced ICT Research Institute, National Institute of Information and Communications Technology, 588-2 Iwaoka, Nishi-ku, Kobe, Hyogo 651-2492, Japan*
2. *PRESTO, Japan Science and Technology Agency, 4-1-8 Honcho, Kawaguchi, Saitama 332-0012, Japan*
*taro@nict.go.jp

Abstract

We report the first development of niobium nitride (NbN)-based ferromagnetic π Josephson junctions. For fabricated NbN/copper-nickel (CuNi)/NbN junctions, we measured the ferromagnetic CuNi thickness and temperature dependences of the Josephson critical current, and found the cusp structure indicating the transition between the 0 and π states. We also observed the characteristic temperature dependences for the junctions with CuNi thicknesses near the 0-π transition thickness, which was originated from the interplay between superconductivity and magnetism. The experimental results are consistently explained by microscopic theory with reasonable physical parameters. The developed NbN-based π junctions are compatible with and provide advantages for superconducting logic circuits and/or quantum computers based on nitride superconductors.

I. INTRODUCTION

In recent years, the novel phenomena caused by an interplay between superconductivity and magnetism, such as the π state and long-range Josephson coupling, have been actively studied [1, 2]. The π state is an interesting quantum state that emerges in ferromagnetic Josephson junctions (Superconductor/Ferromagnet/Superconductor; SFS junctions), and originates from the spatial oscillation of the superconducting order parameter penetrating the ferromagnetic layer [3–11]. In the π state, the difference between the superconducting phases in the two superconductors is π in the ground state, which contrasts with the 0 state in the conventional Josephson junction, where the phase difference is zero in the ground state. Although the possibility of the π state was theoretically predicted many years ago [3, 4], experimental demonstrations of SFS junctions in the π state (π junctions) have been reported during the last fifteen years or so [6–10]. Experimentally, at the transition between the 0 and π states, the Josephson critical current drops to zero and a cusp structure appears in the temperature or ferromagnetic layer's thickness dependences because the "sign" of the critical current is changed at the transition and its absolute values are measured experimentally.

From a device application point of view, π junctions provide advantages in superconducting logic circuits and/or quantum computing devices [12–19]. In logic circuits based on a single-flux-quantum (SFQ) [20], an introduction of a π junction leads to an enhancement of the operation margin and/or a reduction of the cell size in the SFQ circuits [13, 14]. Recently, 0-π state controllable Josephson junctions are expected to be a candidate for the cryogenic memory demanded for superconducting computers [15, 16]. In these structures, the bit states 0 and 1 are saved in the

magnetization of the ferromagnetic layer. As an alternative approach to realize the cryogenic memory, the "φ bit" with the 0- and π-state segments, in which the bit state is recorded in the superconducting phase, has been demonstrated [17]. The π junction also provides an advantage for the superconducting flux quantum bit (qubit); the external magnetic field which is required to introduce the half flux quantum in the superconducting loop can be removed by replacing a conventional Josephson junctions with a π junction [18, 19]. Thus, it is likely that the coherence of the flux qubits can be improved, and a scalability toward large-scale qubits can be improved further.

We adopted niobium nitride (NbN) as an electrode material alternative to niobium (Nb) and aluminum (Al), which are widely used in superconducting logic circuits and qubits. NbN enables high-frequency operation of up to 1.2 THz, and/or operation at around 10 K, because of its superconducting critical temperature (T_C) of around 16 K, which cannot be achieved in superconducting devices made of Nb [21]. We have previously developed superconducting transmon qubits based on fully-epitaxial NbN/AlN/NbN tunnel junctions grown on a magnesium oxide (MgO) substrate, to improve the coherence time of the superconducting qubit [22, 23]. Although the π junctions have thus far been fabricated by using Nb as an electrode [6–10], a (100) NbN film grown on an MgO substrate has a very smooth surface, unlike polycrystalline Nb film. This is a big advantage in realizing a clean superconducting/ferromagnet interface and improving controllability and reproducibility of junction characteristics, but an advanced interfacial control is required because of the relatively short coherence length of NbN of around 4–5 nm.

In this paper, we present NbN-based π junctions and show the dependences of the Josephson critical current on a ferromagnetic copper-nickel (CuNi) barrier thickness and

temperature, for the first time. We demonstrate the distinctive temperature dependence of the junctions with CuNi thicknesses close to the 0-π transition thickness, which is originated from the essential physics of the interaction of the superconductivity and magnetism. It is revealed that all experimental results are consistently explained by microscopic theory with reasonable physical parameters.

II. DEVICE FABRICATION AND EXPERIMENTAL SETUP

In the present work, NbN and CuNi were deposited by the DC magnetron sputtering of a Nb target in Ar and N_2 gases and a $Cu_{0.47}Ni_{0.53}$ target in Ar gas, respectively, at a pressure of 5 mTorr at room temperature. The NbN and CuNi thicknesses were controlled by the sputtering time, using the estimated sputtering rate by Dektak profiler measurements beforehand. The deposited 200-nm thick NbN showed a T_C of 15.1 K and a resistivity of 75 μΩcm at 20 K. By the X-ray diffraction measurements, it was confirmed that the NbN layer was epitaxially grown on MgO substrate with (100) orientation, and thus, a much smoother surface was achieved when compared to the polycrystalline Nb electrodes, which is one of the advantages of a NbN/CuNi interface. In contrast, the NbN on the CuNi layer in an NbN/CuNi/NbN tri-layer will be polycrystalline, unlike the fully-epitaxial NbN/AlN/NbN junctions [22], and the actual roughness of the upper CuNi/NbN interface will be investigated by using the transmission electron microscopy (TEM) in future. To check the magnetic property of the CuNi, we measured the temperature dependence of the in-plane and out-of-plane magnetizations for 30-nm thick CuNi film deposited on the MgO substrate by a commercial SQUID magnetometry system. Our film showed in-plane anisotropy with a Curie temperature (T_{Curie}) of about 200 K. It is known that there is a linear relationship

between T_{Curie} and the Ni concentration x of $Cu_{1-x}Ni_x$ [24], and from this relationship, we expected that $x \lesssim 0.59$ for the deposited CuNi film, which is higher than $x = 0.53$ of the sputtering target [24]. The resistivity of the CuNi film was 50 μΩcm at 4.2 K, which showed good agreement with typical values [8, 10].

We fabricated NbN/CuNi/NbN ferromagnetic Josephson junctions by the following process. First, we deposited tri-layers on a MgO substrate in-situ without breaking vacuum in the same chamber to obtain clean interfaces. The thicknesses of the NbN and CuNi layers were 200 nm and 5.0–11.0 nm, respectively. Next, the pattering was made by an *i*-line stepper system and the tri-layers were etched by CF_4 and Ar gases for NbN and CuNi layers, respectively. Then, the junction part was patterned and the upper NbN and CuNi layers were etched to define the junction area. After evaporating a SiO layer as an insulating layer, we made the contact window at the junction by a lift-off process, and finally deposited and patterned a wiring NbN layer. The junction area of the samples in the present work was 10 μm × 10 μm. Figure 1(a) indicates a picture of the fabricated 10 μm × 10 μm SFS junction and schematics of the cross section of the device.

For the cryogenic measurements of the SFS junctions, we used liquid helium for the CuNi thickness dependence of the Josephson critical current (I_C) at 4.2 K, and the ^{3}He cryocooler system for the temperature dependences of I_C at 0.3–13.0 K. To evaluate I_C, we measured the current-voltage (I-V) characteristics by the standard four-terminal measurement. In SFS junctions, the voltage generated above I_C is very small as sub μV because the normal resistance of the junction (R_n) is comparable with the resistance of the metallic ferromagnet layer if there is a no large additional interfacial resistance. Thus, we adopted the commercial nano-voltmeter (Keysight 34420A) to measure the

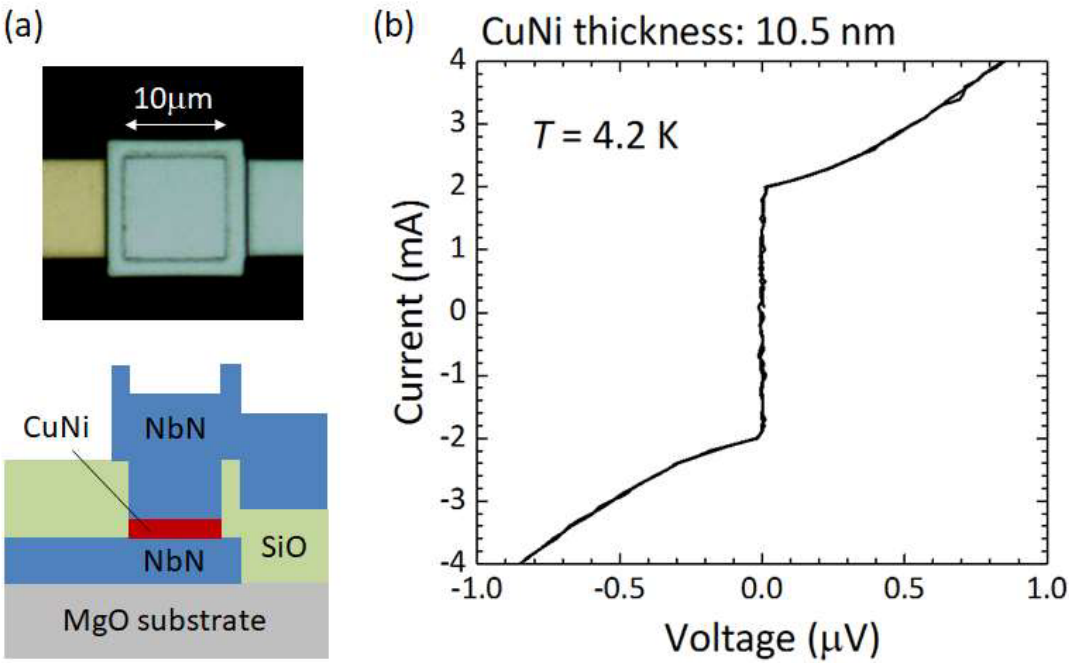

FIG. 1. (a) Picture of the 10 μm × 10 μm SFS junction and schematics of the cross section of the device. (b) Current-voltage characteristics of NbN/CuNi/NbN junction with CuNi thickness of 10.5 nm at 4.2 K.

sub-μV resistance in the present work.

III. RESULTS AND DISCUSSION

Figure 1 (b) shows the typical I-V characteristics of the SFS junction with CuNi thickness of 10.5 nm at 4.2 K. As shown in Fig. 1 (b), a Josephson current with overdamped characteristics was observed, and I_C was estimated to be 2.0 mA. As expected, the generated voltage was very small (sub μV) and the obtained R_n was 254 μΩ. Although the value of R_n is larger than the resistance of 10.5-nm thick CuNi estimated from the resistivity of the single 30-nm thick CuNi film, there seems to be no large interfacial resistances.

To investigate the ground state of the fabricated SFS junctions, we measured I_C for

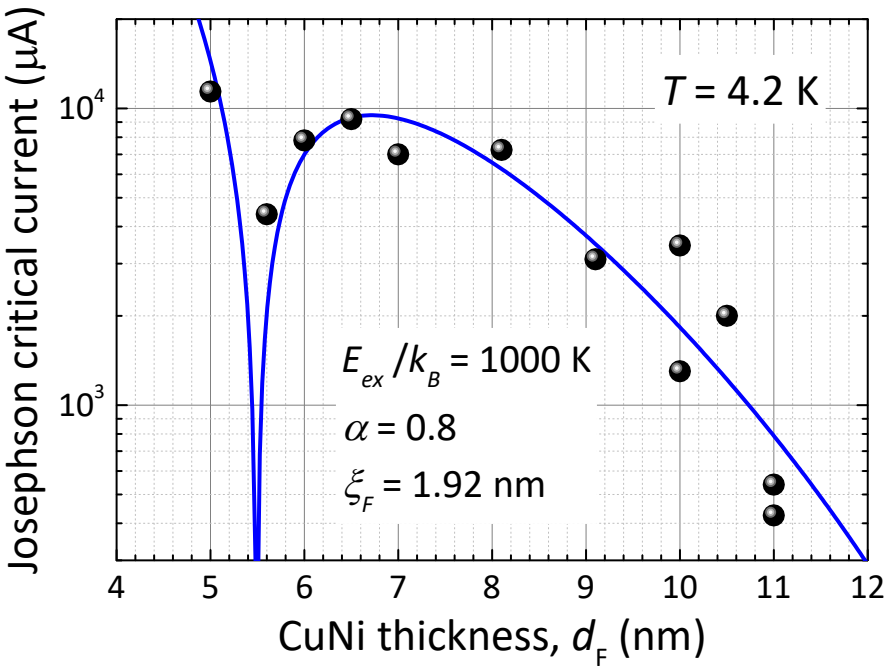

FIG. 2. CuNi thickness dependence of the Josephson critical current of the NbN/CuNi/NbN junctions at 4.2 K. Black symbols indicate the experimental results, and the blue curve indicates the theoretical curve of Eq. (1).

the junctions with CuNi thicknesses (d_F) of 5.0–11.0 nm at 4.2 K. Figure 2 indicates the dependence of I_C on the CuNi thicknesses (black symbols). Although I_C decreases with increasing d_F, a non-monotonic cusp structure that may indicate the 0-π transition was observed around 5.6 nm. A theoretical expression of I_C in the SFS junctions derived from the Usadel equations can be written as functions of d_F and temperature (T) [11]:

$$I_C(d_F,T) = I_{C0}\left(\frac{T}{T_C}\right)\cdot \mathrm{Re}\left(\sum_{n=0}^{\infty}\frac{\mathcal{F}(n)q_1(n)\exp\left(-\frac{q_1(n)d_F}{\xi_F}\right)}{\left(\sqrt{q_2(n)\mathcal{F}(n)+1}+1\right)^2}\right), \qquad (1)$$

where I_{C0} is a constant pre-factor, ξ_F is the coherence length in the ferromagnetic

layer, n is an integer, $q_1(n) = \sqrt{2(i + \alpha + \widetilde{\omega_n})}$, $q_2(n) = (i + \widetilde{\omega_n})/(i + \alpha + \widetilde{\omega_n})$, and $\mathcal{F}(n) = \Delta^2(T)/\left(\omega_n + \sqrt{\omega_n^2 + \Delta(T)^2}\right)^2$ [11]. Here $\Delta(T)$ is the superconducting gap, $\widetilde{\omega_n} = \omega_n/E_{ex} = \pi(2n + 1)k_BT/E_{ex}$, $\alpha = \hbar/(\tau_s E_{ex})$ with the exchange energy E_{ex} and the spin-flip scattering time τ_s in the ferromagnetic layer, the Boltzmann constant k_B, and the Plank constant $\hbar$. The parameter α indicates the degree of the spin-flip scattering effect. The theoretical curve fitted to the experimental result is shown as a blue solid line in Fig. 2. Here we assumed that $E_{ex}/k_B = 1000$ K from the value of CuNi with a close T_{Curie} [25]. To fit the curve to the data, we took the parameters $\alpha = 0.8$, $\xi_F = 1.92$ nm, and $I_{C0} = 6.5\times10^7$ mA. The decay (oscillation) length of the order parameter is expressed as $\xi_{F1(F2)}(T) = \xi_F/\sqrt{\sqrt{1 + (\widetilde{\omega_n} + \alpha)^2} \pm (\widetilde{\omega_n} + \alpha)}$ [25], and from the obtained parameters we derived $\xi_{F1}(0) = 1.33$ nm and $\xi_{F2}(0) = 2.77$ nm.

Here, we discuss the validity of the obtained fitting parameters α, ξ_F, and I_{C0}. When compared to previous work on SFS junctions with a more diluted $Cu_{0.47}Ni_{0.53}$ barrier [9], a weaker spin-flip scattering effect was obtained; $\alpha = 0.8$ (in this work) < 1.33 (in Ref. 9). This is physically reasonable for our case with $x \lesssim 0.59$ in $Cu_{1-x}Ni_x$ because it is known that the spin-flip scattering effect becomes stronger for smaller Ni concentrations [10]. It is also consistent with another work in which a small value of $\alpha = 0.58$ was derived for the relatively stronger ferromagnetic $Cu_{0.4}Ni_{0.6}$ (T_{Curie} = 225 K) [10]. Regarding the coherence length ξ_F of 1.92 nm, the value is intermediate between 1.03 nm and 2.16 nm for the stronger and weaker ferromagnetic CuNi, respectively [9, 10]. Finally, the pre-factor I_{C0} is also reasonable, because the fitted value of 6.5×10^7 mA is comparable to that estimated from the actual physical

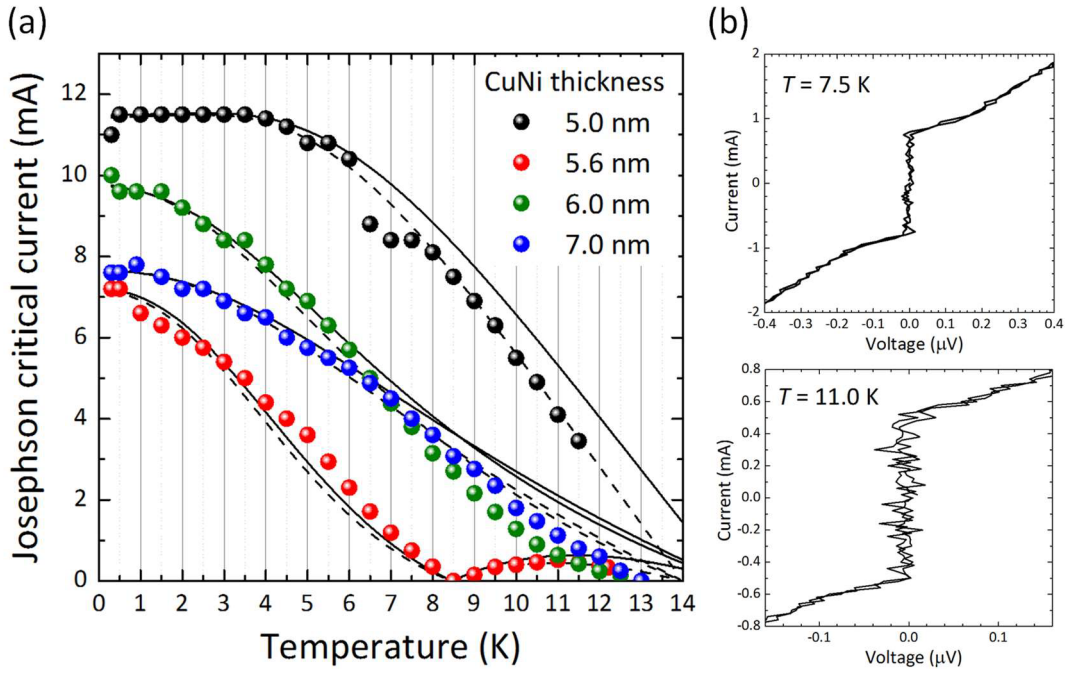

FIG. 3. (a) Temperature dependences of the Josephson critical current of NbN/CuNi/NbN junctions with CuNi thicknesses of 5.0, 5.6, 6.0, and 7.0 nm. The symbols indicate the experimental data, and the solid (dashed) curves indicate theoretical curves of Eq. (1) with T_C = 15.1 (14.0) K. (b) Current-voltage characteristics of the junction with CuNi thickness of 5.6 nm at 7.5 K in the π state and 11.0 K in the 0 state.

parameters such as T_C in the present experiment. Regarding the spread of the experimental data around the theoretical curve in Fig. 2, we expect a slight run-to-run and in-plane variations of the CuNi thickness is a cause as well as the roughness of the upper CuNi/NbN interface.

To confirm the existence of the 0-π transition at around 5.6 nm, we measured the temperature dependences of I_C at 0.3–13.0 K for the junctions with CuNi thicknesses around the cusp; d_F = 5.0, 5.6, 6.0, and 7.0 nm. The symbols and curves shown in Fig. 3 (a) indicate the measured I_C and the theoretical curves, respectively. As we expected

from the CuNi thickness dependence, for the junction with CuNi thickness of 5.6 nm (red symbol), we found a clear temperature-induced 0-π transition with a cusp structure at around 8.5 K. When the CuNi thickness is close to the critical thickness of the 0-π transition, the quantum state changes from the π state at lower temperatures to the 0 state at higher temperatures, caused by the increase of the oscillation length $\xi_{F2}(T)$ as the temperature increases. Owing to the high T_C of NbN, we could observe the 0-π transition at the relatively high temperature of 8.5 K, whereas the temperature-induced 0-π transitions at the lower temperatures of around 2–4 K have been reported for conventional Nb-based SFS junctions [6, 8–10]. Figure 3 (b) shows I-V characteristics at 7.5 K in the π state and 11.0 K in the 0 state.

Furthermore, we observed the characteristic temperature dependences for junctions with neighboring CuNi thicknesses of 5.0, 6.0, and 7.0 nm. In the junction with 5.0-nm thick CuNi (black symbol), the 0 state remains throughout the whole temperature range, and I_C showed a flat temperature dependence for a wide temperature range of 0.3–5.0 K. This distinctive flat I_C dependence originates from the competition between the increase of the oscillation period (increase of I_C) and decrease of the Cooper pair density (decrease of I_C) as the temperature increases [10]. In contrast, both junctions with CuNi thicknesses of 6.0 nm (green symbol) and 7.0 nm (blue symbol) were in the π state at all temperatures. It is striking that the temperature dependence for the 6.0-nm CuNi showed a steeper slope than that for the 7.0 nm CuNi, and the crossover of I_C appeared at around 7 K. This is because the junction with 6.0-nm CuNi is located close to the 0-π transition thickness (~5.6 nm) and thus I_C decreases rapidly when the oscillation period increases with the temperature increases. Conversely, the 7.0-nm CuNi junction is far from the transition thickness, and so I_C changes relatively slowly compared to that for

the 6.0-nm CuNi junction.

These characteristic behaviors can be reproduced quantitatively by using the microscopic theory [11]. The solid lines shown in Fig. 3 (a) indicate the curves of Eq. (1) with $E_{ex}/k_B = 1000$ K, $\alpha = 0.8$, $\xi_F = 1.923$ nm, and T_C = 15.1 K as common parameters for all CuNi thicknesses and with $I_{C0} = 4.5\times10^7 - 13.4\times10^7$ mA as the one free parameter. Here we assumed a temperature-independent E_{ex} because T_{Curie} is much larger than T_C in the present experiment [26]. As shown in the figure, the theoretical curves follow the experimental results well, although there are some deviations at high temperature region, and the curves show the characteristic temperature dependences discussed above. It should be noted that both the CuNi thickness dependence (Fig. 2) and the temperature dependence for all CuNi thicknesses can be consistently explained by one parameter set of E_{ex}, α, and ξ_F. Regarding the deviation of the theoretical curves from the experimental data at higher temperatures, we found that T_C of the top wiring NbN on the SiO layer was reduced to 13.4 K in the samples, and thus I_C dropped to zero before reaching 15.1 K. Although it is difficult to evaluate the actual T_C of the counter and base NbN layers of the junction, the theoretical curves from the assumption of a reduced T_C of 14.0 K are shown in the dashed lines in Fig. 3 (a). The calculated curves followed the experimental results well even at higher temperature region.

From the above experimental results and theoretical analysis, we convinced that NbN-based π junctions were obtained for CuNi thicknesses of above 5.6 nm. As shown in Fig. 3 (a), the NbN-based junctions can work as a π phase shifter by setting the CuNi thickness, not only for superconducting qubits operated at sub-Kelvin temperatures, but also for superconducting logic circuits operated at high temperatures of around 10 K.

Furthermore, it is noteworthy that the developed NbN-based junction showed a high critical current density (j_C) of around 10,000 A/cm^2 in the π state for the junctions with 6.0- and 6.5-nm-thick CuNi barrier (see also Fig. 2). The obtained j_C is ten times larger than that reported for Nb-based π junction [9]. This feature will provide advantages to the various superconducting device applications such as the SFQ circuit. In the application of the cryogenic memory based on the Josephson φ junction, the NbN-based π junctions are expected to provide various merits such as a reduction of the memory element size because of their small Josephson penetration length [17]. From the point of view of the superconducting π qubit [18,19], the NbN-based π junction is a good compatibility with nitride-based qubits, which is expected to be a good-coherence qubit (e.g. Ref. 23). Even though the π junction itself is not fully epitaxial, a fabrication process and a device structure become simpler by adopting the NbN-based π junction as a phase shifter.

IV. CONCLUSION

In conclusion, we succeeded in fabricating an NbN-based π junction for the first time, and precisely measured and analyzed the dependence of the Josephson critical current on the ferromagnetic CuNi thickness and temperature. We observed a distinctive temperature dependence of the CuNi thickness close to the 0-π transition thickness, as well as the temperature-induced 0-π transition, reflecting the oscillation of the order parameter in the CuNi due to the interaction of superconductivity and magnetism. The experimental results were consistently explained by the microscopic theory, with reasonable physical parameters. The results presented in this paper provide not only a deeper understanding of the physics of superconducting spintronics, but reveal a new

material choice for realizing high-performance superconducting classical/quantum devices.

ACKNOWEDGMENTS

This work was supported by JST PRESTO Grant Number JPMJPR1669, Japan. The authors thank T. Seki, S. Hikino, and S. Kawabata for fruitful discussions.

REFERENCES

[1] J. Linder and J. W. A. Robinson, Superconducting spintronics, Nat. Phys. **11**, 307 (2015).
[2] M. Eschrig, Spin-polarized supercurrents for spintronics, Physics Today. **64**, 43 (2011).
[3] L. N. Bulaevskii, V. V. Kuzii, and A. A. Sobyanin, Superconducting system with weak coupling to the current in the ground state, JETP Lett. **25**, 290 (1977).
[4] A. I. Buzdin, L. N. Bulaevskii, and S. V. Panyukov, Critical-current oscillations as a function of the exchange field and thickness of the ferromagnetic metal (*F*) in an *S*-*F*-*S* Josephson junciton, JETP Lett. **35**, 178 (1982).
[5] E. A. Demler, G. B. Arnold, and M. R. Beasley, Superconducting proximity effects in magnetic metals, Phys. Rev. B. **55**, 15174 (1997).
[6] V. V. Ryazanov, V. A. Oboznov, A. Yu. Rusanov, A. V. Veretennikov, A. A. Golubov, and J. Aarts, Coupling of Two Superconductors through a Ferromagnet: Evidence for a π Junction, Phys. Rev. Lett. **86**, 2427 (2001).
[7] T. Kontos, M. Aprili, J. Lesueur, F. Genêt, B. Stephanidis, and R. Boursier, Josephson Junction through a Thin Ferromagnetic Layer: Negative Coupling, Phys. Rev. Lett. **89**, 137007 (2002).
[8] H. Sellier, C. Baraduc, F. Lefloch, and R. Calemczuk, Temperature-induced crossover between 0 and π states in S/F/S junctions, Phys. Rev. B. **68**, 054531 (2003).
[9] V. A. Oboznov, V. V. Bol'ginov, A. K. Feofanov, V. V. Ryazanov, and A. I. Buzdin, Thickness Dependence of the Josephson Ground States of Superconductor-Ferromagnet-Superconductor Junctions, Phys. Rev. Lett. **96**, 197003 (2006).

[10] M. Weides, M. Kemmler, E. Goldobin, D. Koelle, R. Kleiner, H. Kohlstedt, and A. Buzdin, High quality ferromagnetic 0 and π Josephson tunnel junctions, Appl. Phys. Lett. **89**, 122511 (2006).
[11] A. I. Buzdin, Proximity effects in superconductor-ferromagnet heterostructures, Rev. Mod. Phys. **77**, 935 (2005).
[12] T. Yamashita and H. Terai, Recent Progress in Ferromagnet/Superconductor Hybrid Structure and its Applications to Cryogenic Computing, IEEJ Trans. Fundam. Mater. **136**, 728 (2016).
[13] A. V. Ustinov and V. K. Kaplunenko, Rapid single-flux quantum logic using π-shifters, J. Appl. Phys. **94**, 5405 (2003).
[14] A. K. Feofanov, V. A. Oboznov, V. V. Bol'ginov, J. Lisenfeld, S. Poletto, V. V. Ryazanov, A. N. Rossolenko, M. Khabipov, D. Balashov, A. B. Zorin, P. N. Dmitriev, V. P. Koshelets, and A. V. Ustinov, Implementation of superconductor/ferromagnet/superconductor π-shifters in superconducting digital and quantum circuits, Nat. Phys. **6**, 593 (2010).
[15] B. Baek, W. H. Rippard, S. P. Benz, S. E. Russek, and P. D. Dresselhaus, Hybrid superconducting-magnetic memory device using competing order parameters, Nat. Commun. **5**, 3888 (2014).
[16] E. C. Gingrich, B. M. Niedzielski, J. A. Glick, Y. Wang, D. L. Miller, R. Loloee, W. P. Pratt Jr, and N. O. Birge, Controllable 0–π Josephson junctions containing a ferromagnetic spin valve, Nat. Phys. **12**, 564 (2016).
[17] E. Goldobin, H. Sickinger, M. Weides, N. Ruppelt, H. Kohlstedt, R. Kleiner, and D. Kolle, Memory cell based on a φ Josephson junction, Appl. Phys. Lett. **102**, 242602 (2013).
[18] T. Yamashita, K. Tanikawa, S. Takahashi, and S. Maekawa, Superconducting π Qubit with a Ferromagnetic Josephson Junction, Phys. Rev. Lett. **95**, 097001 (2005).
[19] T. Yamashita, S. Takahashi, and S. Maekawa, Superconducting π qubit with three Josephson Junctions, Appl. Phys. Lett. **88**, 132501 (2006).
[20] K. K. Likharev and V. K. Semenov, RSFQ Logic/Memory Family: A New Josephson-Junction Technology for Sub-Terahertz-Clock-Frequency Digital Systems, IEEE Trans. Appl. Supercond. **1**, 3 (1991).
[21] K. Makise, H. Terai, S. Miki, T. Yamashita, and Z. Wang, Design and Fabrication of All-NbN SFQ Circuits for SSPD Signal Processing, IEEE Trans. Appl. Supercond. **23**, 1100804 (2013).
[22] Z. Wang, H. Terai, W. Qiu, K. Makise, Y. Uzawa, K. Kimoto, and Y. Nakamura, High-quality epitaxial NbN/AlN/NbN tunnel junctions with a wide range of current

density, Appl. Phys. Lett. **102**, 142604 (2013).
[23] Y. Nakamura, H. Terai, K. Inomata, T. Yamamoto, W. Qiu, and Z. Wang, Superconducting qubits consisting of epitaxially grown NbN/AlN/NbN Josephson junctions, Appl. Phys. Lett. **99**, 212502 (2011).
[24] A. Rusanov, R. Boogaard, M. Hesselberth, H. Sellier, and J. Aarts, Inhomogeneous superconductivity induced in a weak ferromagnet, Physica C. **369**, 300 (2002).
[25] A. S. Vasenko, A. A. Golubov, M. Yu. Kupriyanov, and M. Weides, Properties of tunnel Josephson junctions with a ferromagnetic interlayer, Phys. Rev. B. **77**, 134507 (2008).
[26] M. Mori, S. Hikino, S. Takahashi, and S. Maekawa, Role of Magnetic Scattering in 0–π Transitions in a Superconductor/Ferromagnetic Metal/Superconductor Junction, J. Phys. Soc. Jpn. **76**, 054705 (2007).